Available online at www.sciencedirect.com
ScienceDirect
Thermochimica Acta 453 (2007) 128–135
thermochimica acta
www.elsevier.com/locate/tca

Thermal waves scattering by a subsurface sphere in a semi-infinite exponentially graded material using non-Fourier's model

X.Q. Fang [a,*], C. Hu [b]

[a] *Department of Aerospace Engineering & Mechanics, Harbin Institute of Technology, Harbin 150001, China*
[b] *School of Aerospace Engineering and Mechanics, Tongji University, Shanghai 200092, China*

Received 4 July 2006; received in revised form 16 November 2006; accepted 19 November 2006
Available online 25 November 2006

Abstract

In this study, the multiple scattering of thermal waves and temperature distribution resulting from a subsurface sphere in a semi-infinite exponentially graded material are investigated, and the analytical expression of the temperature at the surface of the graded material is obtained. Non-Fourier heat conduction equation is applied to solve the temperature at the surface, and the image method is used to satisfy the semi-infinite boundary condition of graded material. The thermal wave fields are expressed using wave function expansion method, and the expanded mode coefficients are determined by satisfying the boundary condition of the sphere. According to the wave equation of heat conduction, a general solution of scattered thermal waves is presented for the first time. The temperature distribution and phase difference at the surface of the semi-infinite material with different parameters are graphically presented. Analyses show that the hyperbolic heat conduction equation cannot be regarded as a continuation of the parabolic heat conduction equation at very short time scale. The effects of the incident wave number, the structural and physical parameters on the distribution of temperature and phase difference in the semi-infinite material are also examined.

Keywords: Non-Fourier heat conduction law; Multiple scattering of thermal waves; Semi-infinite exponentially graded materials; Sphere defect; Image method

1. Introduction

The classical Fourier's law is quite accurate for most common engineering situations. However, for situations involving very short times, Fourier's law noticeably breaks down. So, non-Fourier heat conduction law was developed. The wave models, which can describe the relaxation behavior of heat conduction, are the modification for classical theory of Fourier heat conduction. When the equations of heat conduction and energy are incorporated, the hyperbolic equation of heat conduction can be obtained. In many cases (e.g., laser heating, multilayer insulation at the low temperature, superconducting film, etc.), non-Fourier heat conduction is encountered. When the wavelength of the heat carrier is comparable to the characteristic length of structures, or the time of heat conduction is not equal to the time for reaching thermal equilibrium, the heat conduction in structures expresses wave nature. In the situation involving temperature near absolute zero or extreme thermal gradients, the concept of the complex heat capacity can be used to describe an internal relaxation in the system, as well as the non-Fourier heat conduction law. But the latter can be used only for the case of the exponential relaxation when the both approaches are equivalent [1–3].

Functionally graded materials (FGMs) are a new generation of engineering materials wherein the micro-structural details are spatially varied through non-uniform distributions of the reinforcement phases, by using reinforcements with different properties, sizes and shapes, as well as by interchanging the roles of reinforcement and matrix phases in a continuous manner [4]. For example, ceramics are useful in high strength and temperature applications. However, they suffer from low toughness. In an ideal FGM, they may be combined in an intelligent manner with a metal of high toughness to raise the toughness of the combination.

Computational analysis is an effective method for designing specified FGM systems and understanding the behavior of FGMs. For homogeneous medium, boundary integral equation methods have been applied extensively. However, the formulation of integral equations relies on the fundamental solution of partial differential equation. Application of the boundary

* Corresponding author. Tel.: +86 451 86410268.
E-mail address: fangxueqian@163.com (X.Q. Fang).

0040-6031/$ – see front matter © 2006 Elsevier B.V. All rights reserved.
doi:10.1016/j.tca.2006.11.014

integral technique has therefore been limited to homogeneous or piecewise homogeneous media. Applying boundary integral equation methods, Gray et al. investigated the heat conduction of exponentially graded materials, Green's functions in free space were derived, the closed-form solution for steady-state diffusion equation was also obtained in two and three dimension spaces [5].

Using the superfluid liquid helium, Peshkov firstly discovered the existence of thermal waves in the medium when the temperature is close to absolute zero degree in experiment [6]. Subsequently, C. Cattaneo proposed the model of thermal waves [7]. Qiu and Tien studied the microscopic radiation during the short-pulse laser heating in solid materials [8]. Based on dual-phase-lag concept, Tzou constructed a universal constitutive equation between the heat flux vector and the temperature gradient. He considered the interactions between waves and phonon–electron as the diffusion of phonon, and the experiment was also presented to prove the lagging behavior of thermal wave propagation [9]. Kvrner and Bergmann pointed out that with the advent of ultrashort pulse lasers, because the time of material processing is relatively short, and the influence of thermal waves during the heat conduction becomes prominent, the hyperbolic equation of heat conduction should be employed to compute and analyze this problem [10].

Base on the equation of thermal diffusion, Terron et al. studied the multiple scattering of thermal waves between the subsurface cylinder and the material surface, theoretical analysis and experimental investigation were carried out, and the general solution for the multiple scattering of thermal waves was also presented [11]. Applying the diffusive model of heat conduction, Thibaud et al. presented the theoretical and numerical results for the multiple scattering of a diffusive wave resulting from an object embedded in a semi-infinite substrate [12]. Terron et al. gave us the analyses and experiment of the multiple scattering of a plane thermal wave between a two-layer subsurface cylinder and the material surface [13]. Salazar and Sanchez-Lavega presented a general solution for the ac temperature field of an opaque material containing aligned subsurface cylinders produced by a modulated line illumination [14].

Different physical parameters and boundary conditions of subsurface have great effects on the propagation and diffusion of thermal waves, which is directly presented by the temperature field at the surface of materials. By using the detecting system of thermal waves and measuring the changes of temperature at the surface of materials, the internal structures can be obtained for purpose of detection and inspection [13]. The nondestructive detection technology is of considerable importance in the research of designing new materials in aerospace engineering, and improving the reliability of industrial products and facilities.

To the author's knowledge, up to present time the physical models employed to determine the temperature distribution of the sample with defects in infrared thermal imaging are still based on the classical Fourier heat conduction law. Namely, parabolic equation of heat diffusion is often applied to compute and analyze this problem [15]. The main objective of this paper is to investigate the multiple scattering of thermal waves and temperature distribution resulting from an embedded sphere defect in a semi-infinite exponentially graded material. The thermal waves are generated at the surface of opaque material by a modulated optical beam. The sphere defect is taken as a sphere cavity under thermal insulation condition. Based on non-Fourier heat conduction law, the hyperbolic equation of heat conduction is solved by employing wave function expansion method. The temperature distribution and phase difference at the surface of the semi-infinite material under different parameters are graphically presented. The effects of the incident wave number, the structural and physical parameters on the temperature distribution and phase difference are also examined.

2. Wave motion equation of thermal waves and its solution

Consider a semi-infinite exponentially graded material, as depicted in Fig. 1. A thermally insulated sphere defect with adiabatic surface of radius a is embedded in the materials. The depth of the center of sphere defect beneath the surface is b. Let an ultrashort laser pulse modulated at a frequency of f hit at the surface of heated materials along the z direction. The thermal waves are generated in the materials. Based on the non-Fourier law of heat conduction, the governing equation of temperature in the materials, as utilized in previous investigation [16], can be written as

$$\nabla \cdot (\lambda \nabla T) = \rho c_p \left(\frac{\partial T}{\partial t} + \tau \frac{\partial^2 T}{\partial t^2} \right) \tag{1}$$

where ∇ is the Hamilton operator and $\nabla = \mathrm{i}\partial/\partial x + \mathrm{j}\partial/\partial y + \mathrm{k}\partial/\partial z$, λ, c_p and ρ are the thermal conductivity, the specific heat at constant pressure and the density, respectively, T the temperature in graded materials, and τ is the exponential relaxation time needed for reaching new equilibrium. It should be noted that the exponential relaxation time is a thermodynamic property of the materials.

For simplicity, the density of materials and relaxation time are assumed to be constants. The shear modulus and density of materials vary continuously, and the same non-homogeneity

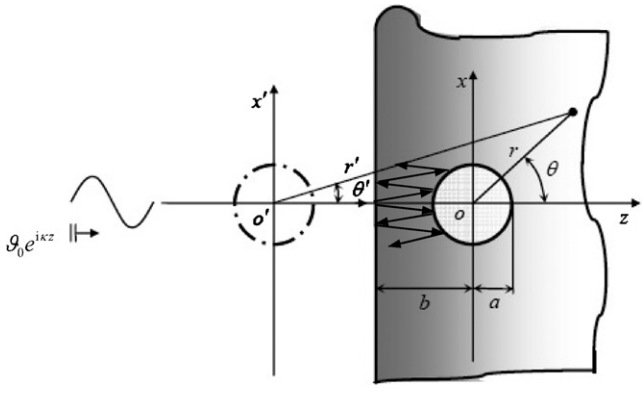

Fig. 1. Geometry and coordinates used to study the multiple scattering of a subsurface sphere embedded in a semi-infinite graded material.

parameter is used to describe the variation of them, i.e.,

$$\lambda = \mathrm{Re}[\lambda_0 \exp(2\sigma z)], \qquad c_p = \mathrm{Re}[c_{p0} \exp(2\sigma z)], \tag{2}$$

Here λ_0, c_{p0} are complex parameters, and denote the complex thermal conductivity and the specific heat at a constant pressure when $z = 0$, respectively. σ is the spatial variational exponent of physical parameters, and denotes the nonhomogeneous parameter of materials. It may be a complex variable, i.e., $\sigma = \sigma_1 + \mathrm{i}\sigma_2$.

Substituting Eqs. (2) into (1), the following equation can be obtained:

$$\nabla^2 T + 2\sigma \frac{\partial T}{\partial z} = \frac{1}{c^2}\frac{\partial^2 T}{\partial t^2} + \frac{1}{D}\frac{\partial T}{\partial t}, \tag{3}$$

where D ($D = \lambda/\rho c_p$) is the thermal diffusivity, and c is the propagating speed of thermal waves at high frequencies, $c = \sqrt{D/\tau}$. According to Eq. (2), the thermal diffusivity of graded materials is a constant.

The solution of periodic steady state is investigated. Suppose that $T = T_0 + \mathrm{Re}[\vartheta \exp(-\mathrm{i}\omega t)]$, the following equation can be derived in terms of Eq. (3):

$$\nabla^2 \vartheta + 2\sigma \frac{\partial \vartheta}{\partial z} + \left(\frac{\omega^2}{c^2} + \frac{\mathrm{i}\omega}{D}\right)\vartheta = 0, \tag{4}$$

where T_0 is the average temperature, and ω is the incident frequency with $\omega = 2\pi f$.

Thus, the solution of Eq. (4) takes the following form:

$$\vartheta = \exp(-\sigma z) u(x, y, z), \tag{5}$$

in which the function $u(x, y, z)$ should satisfy the following equation:

$$\nabla^2 u + \kappa^2 u = 0, \tag{6}$$

where κ is the wave number of complex variables, $\kappa = ((\omega^2/c^2) + (\mathrm{i}\omega/D) - \sigma^2)^{1/2} = \alpha + \mathrm{i}\beta$, and α, β are the wave number and absorption coefficient of thermal waves, respectively. Without loss of generality, after normalizing and taking $\alpha > 0$, $\beta > 0$, one can obtain:

Here k is the wave number of thermal waves without diffusive effect.

Note that when the propagation speed of thermal waves is $c \to \infty$ and the nonhomogeneous parameter is $\sigma \to 0$, one can obtain $\alpha \to \sqrt{(1/2)(\omega/D)} = 1/\mu$ and $\beta \to \sqrt{(1/2)(\omega/D)} = 1/\mu$. So, the wave number of thermal waves is $\kappa = \alpha + \mathrm{i}\beta \to (1 + i)(1/\mu)$. By this way, the hyperbolic equation of heat conduction in graded materials can be reduced to the classical equation of Fourier heat conduction.

According to Eqs. (6)–(8), one can see that in FGMs there exists the wave motion with the form of $\vartheta\, \mathrm{e}^{-\mathrm{i}\omega t} = \vartheta_0 \exp[-(\beta + \sigma)z]\, \mathrm{e}^{\mathrm{i}(\alpha z - \omega t)} = \vartheta_0 \exp[-(\beta + \sigma_1)z]\, \mathrm{e}^{\mathrm{i}[(\alpha - \sigma_2 z - \omega t)]}$. The wave modes denote the propagating thermal waves with its amplitude of vibration attenuating in the z direction. The existing condition of the stable propagating waves which propagate in the positive z direction is $\sigma_1 > \beta$ and $\sigma_2 < \alpha$.

The general solution of the scattered field of thermal waves in graded materials determined by Eq. (4) can be described as [17,18]

$$\vartheta = \mathrm{e}^{-\sigma z} \sum_{n=0}^{\infty} \sum_{m=-n}^{n} A_{mn} h_n^{(1)}(\kappa r) P_n^m(\cos\theta)\, \mathrm{e}^{\mathrm{i}m\varphi}, \tag{9}$$

where $h_n^{(1)}(\cdot)$ is the spherical Hankel function, $h_n^{(1)}(x) = \sqrt{\pi/2x} H_{n+(1/2)}^{(1)}(x)$, $H_n^{(1)}(\cdot)$ is the Hankel function of the first kind, A_{nm} are the mode coefficients resulting from the subsurface sphere defect, and are determined by the boundary conditions, $P_n^m(\cdot)$ is the associated Legendre polynomial, and $P_n^m(x) = (1/2^n n!)(1 - x^2)^{m/2}(\mathrm{d}^{m+n}/\mathrm{d}x^{m+n})(x^2 - 1)^n$. Note that the temperature is independent of φ due to the symmetry, so it is suppressed in all subsequent representations for notational convenience.

3. The incidence of thermal waves and total wave field

Thermal waves can be generated at the surface of graded materials by the laser beam with modulated ultrashort pulse. Let a periodic stable thermal wave propagate along the positive

$$\alpha = \sqrt{\frac{1}{2}\left\{\sqrt{\left[\frac{\omega^2}{c^2} - (\sigma_1^2 - \sigma_2^2)\right]^2 + \left(\frac{\omega}{D} - 2\sigma_1\sigma_2\right)^2} + \frac{\omega^2}{c^2} - (\sigma_1^2 - \sigma_2^2)\right\}}$$

$$= \sqrt{\frac{1}{2}\left\{\sqrt{k^2 - (\sigma_1^2 - \sigma_2^2)^2 + 4\left(\frac{1}{\mu^2} - \sigma_1\sigma_2\right)^2} + [k^2 - (\sigma_1^2 - \sigma_2^2)]\right\}} \tag{7}$$

$$\beta = \sqrt{\frac{1}{2}\left\{\sqrt{\left[\frac{\omega^2}{c^2} - (\sigma_1^2 - \sigma_2^2)\right]^2 + \left(\frac{\omega}{D} - 2\sigma_1\sigma_2\right)^2} - \frac{\omega^2}{c^2} + (\sigma_1^2 - \sigma_2^2)\right\}}$$

$$= \sqrt{\frac{1}{2}\left\{\sqrt{[k^2 - (\sigma_1^2 - \sigma_2^2)]^2 + 4\left(\frac{1}{\mu^2} - \sigma_1\sigma_2\right)^2} - [k^2 - (\sigma_1^2 - \sigma_2^2)]\right\}} \tag{8}$$

z direction. The incident plane thermal wave can be expanded in a series of spherical waves by using spherical Bessel functions of the first kind $j_n(\cdot)$ and the Legendre functions $P_n(\cdot)$, i.e. [19]

$$\begin{aligned}\vartheta_1^{(\mathrm{i})} &= \vartheta_0 \exp(\mathrm{i}\kappa b)\exp(-\sigma z)\exp[\mathrm{i}(\kappa z-\omega t)]\\ &= \vartheta_0 \exp(\mathrm{i}\kappa b)\exp(-\sigma z)\sum_{n=0}^{\infty}(2n+1)i^n\\ &\quad\times j_n(\kappa r)P_n(\cos\theta)\exp(-\mathrm{i}\omega t)\end{aligned} \tag{10}$$

where ϑ is the temperature amplitude of incident thermal waves, and κ is the wave number of incident waves. Note that $P_n(x) = P_n^0(x) = (1/2^n n!)(\mathrm{d}^n/\mathrm{d}x^n)(x^2-1)^n$.

The reflected waves at the surface of the semi-infinite material can be described by the virtual image. For the image sphere, the thermal waves propagate in the negative z' direction, and are described as

$$\begin{aligned}\vartheta_2^{(\mathrm{i})} &= \vartheta_0 \exp(\mathrm{i}\kappa b)\exp(\sigma z')\exp[-\mathrm{i}(\kappa z'+\omega t)]\\ &= \vartheta_0 \exp(\mathrm{i}\kappa b)\exp(\sigma z')\sum_{n=0}^{\infty}(2n+1)i^{-n}\\ &\quad\times j_n(\kappa r')P_n(\cos\theta')\exp(-\mathrm{i}\omega t)\end{aligned} \tag{11}$$

In the local spherical coordinate system (r, θ, φ) of the real sphere, the scattered field of thermal waves resulting from the subsurface sphere can be described as

$$\vartheta_1^{(s)} = \exp(-\sigma r\cos\theta)\sum_{n=0}^{\infty}A_n^1 h_n^{(1)}(\kappa r)P_n(\cos\theta)\exp(-\mathrm{i}\omega t). \tag{12}$$

Likewise, in the local spherical polar coordinate (r', θ', φ') of the image sphere, the scattered field resulting from the image sphere can be written as

$$\begin{aligned}\vartheta_2^{(\mathrm{s})} &= \exp(\sigma z')\sum_{n=0}^{\infty}B_n^1 h_n^{(1)}(\kappa r')P_n(\cos\theta')\exp(-\mathrm{i}\omega t)\\ &= \exp(\sigma r'\cos\theta')\sum_{n=0}^{\infty}(-1)^n A_n^1 h_n^{(1)}(\kappa r')P_n(\cos\theta')\exp(-\mathrm{i}\omega t),\end{aligned} \tag{13}$$

where A_n^l, B_n^l, $(l = 1, 2, \ldots, \infty)$ are the lth mode coefficients of thermal waves of the real and image spheres, respectively. They can be determined by satisfying the boundary condition of the subsurface sphere.

Thus, the total wave field in graded materials is taken to be the superposition of the incident waves, the scattered waves and the reflected waves at the surface, i.e.,

$$\vartheta = \vartheta_1^{(\mathrm{i})} + \vartheta_1^{(\mathrm{s})} + \vartheta_2^{(\mathrm{s})}. \tag{14}$$

In this paper, the case that the boundary condition of the subsurface sphere is adiabatic is studied. By using the temperature function, it can be expressed as the following form:

$$\left.\frac{\partial\vartheta}{\partial\mathbf{n}}\right|_a = -\left.\frac{\partial\vartheta}{\partial r}\right|_a = 0, \tag{15}$$

Here **n** denotes the out normal of the boundary of subsurface sphere.

4. Determinant of mode coefficients and solution for temperature at the surface

By satisfying the boundary condition of the subsurface sphere, the mode coefficients of thermal waves can be determined. Substituting Eqs. (14) into (15), the following expressions can be derived:

$$\sum_{n=-\infty}^{\infty}E_n^l X_n^l = E^l, \quad l = 1, 2, \ldots, \infty, \tag{16}$$

where

$$\begin{aligned}E_n^1 &= \exp(-\sigma a\cos\theta)\{\sigma\cos\theta h_n^{(1)}(\kappa a) - \frac{\kappa}{2n+1}[nh_{n-1}^{(1)}(\kappa a)\\ &\quad -(n+1)h_{n+1}^{(1)}(\kappa a)]\}P_n(\cos\theta),\end{aligned} \tag{17}$$

$$E^1 = -\vartheta_0(\sigma-\mathrm{i}\kappa)\cos\theta\exp(\mathrm{i}\kappa b)\exp[-(\sigma-\mathrm{i}\kappa)a\cos\theta], \tag{18}$$

$$\begin{aligned}E_n^2 &= \exp(-\sigma a\cos\theta')\{\sigma\cos\theta' h_n^{(1)}(\kappa a) - \frac{\kappa}{2n+1}[nh_{n-1}^{(1)}(\kappa a)\\ &\quad -(n+1)h_{n+1}^{(1)}(\kappa a)]\}P_n(\cos\theta'),\end{aligned} \tag{19}$$

$$\begin{aligned}E^2 &= \sum_{n=0}^{\infty}(-1)^n A_n^1\exp(\sigma r'\cos\theta')\{\sigma\cos\theta' h_n^{(1)}(\kappa r')\\ &\quad +\frac{\kappa}{2n+1}[nh_{n-1}^{(1)}(\kappa r') - (n+1)h_{n+1}^{(1)}(\kappa r')]\}P_n(\cos\theta'),\end{aligned} \tag{20}$$

$$\begin{aligned}E_n^l &= \exp(-\sigma a\cos\theta)\{\sigma\cos\theta h_n^{(1)}(\kappa a)\\ &\quad -\frac{\kappa}{2n+1}[nh_{n-1}^{(1)}(\kappa a) - (n+1)h_{n+1}^{(1)}(\kappa a)]\}P_n(\cos\theta),\end{aligned} \tag{21}$$

$$\begin{aligned}E^l &= \sum_{n=0}^{\infty}(-1)^n A_n^{l-1}\exp(\sigma r'\cos\theta')\{\sigma\cos\theta' h_n^{(1)}(\kappa r')\\ &\quad +\frac{\kappa}{2n+1}[nh_{n-1}^{(1)}(\kappa r') - (n+1)h_{n+1}^{(1)}(\kappa r')]\}P_n(\cos\theta'),\end{aligned} \tag{22}$$

with $r' = \sqrt{a^2+4b^2+4ab\cos\theta}$, $\theta' = \arccos[(2b + a\cos\theta)/r']$, $X_n^l = A_n^l$.

Multiplying by $P_j(\cos\theta)\sin\theta$ on both sides of Eq. (16) and integrating from 0 to π, yield the following infinite algebraic equations:

$$\sum_{n-0}^{\infty}E_{nj}^l X_n^l = E_j^l, \quad j = n = 0, 1, 2, \ldots, \infty, \tag{23}$$

where

$$E_{nj}^{l} = \frac{2j+1}{2}\int_{0}^{\pi} E_{n}^{l} P_{j}(\cos\theta)\sin\theta\,\mathrm{d}\theta = \frac{2j+1}{2}\int_{-1}^{1} E_{n}^{l} P_{j}(x)\,\mathrm{d}x, \tag{24}$$

$$E_{j}^{l} = \frac{2j+1}{2}\int_{0}^{\pi} E^{l} P_{j}(\cos\theta)\sin\theta\,\mathrm{d}\theta = \frac{2j+1}{2}\int_{-1}^{1} E^{l} P_{j}(x)\,\mathrm{d}x. \tag{25}$$

Eq. (23) are the infinite algebraic equations determining the mode coefficients of thermal waves.

So, the expression of the temperature distribution at the surface of graded materials can be expressed as

$$\begin{aligned}\vartheta = {} & \vartheta_0 \exp(\mathrm{i}\kappa b)\exp(-\sigma z)\exp(\mathrm{i}\kappa z)\exp(-\mathrm{i}\omega t) \\ & + \exp(-\sigma z)\sum_{l=1}^{\infty}\sum_{n=0}^{\infty} A_{n}^{l} h_{n}^{(1)}(\kappa r) P_{n}(\cos\theta)\exp(-\mathrm{i}\omega t) \\ & + \exp(\sigma z')\sum_{l=1}^{\infty}\sum_{n=0}^{\infty}(-1)^{n} A_{n}^{l} h_{n}^{(1)}(\kappa r') P_{n}(\cos\theta')\exp(-\mathrm{i}\omega t),\end{aligned} \tag{26}$$

Here $\theta = \pi - \arccos[(r\sin\theta')/b]$, $y' = y = r\sin\theta\sin\varphi$, $\theta' = \arccos[(r\sin\theta)/b]$, and $y = 0$–4.

If there exists defect in the materials, multiple scattering of thermal waves between the subsurface sphere and the surface will occur, which influences the distribution of temperature at the surface of graded materials. Periodic heating will bring about the temperature variation inside the materials. By making using of the variation of temperature amplitude and the phase difference resulting from the defect, imaging of thermal waves can be obtained. By measuring the temperature variation at the surface of materials, the defect embedded beneath the surface can be estimated and evaluated.

5. Numerical examples and discussions

In the following analysis it is convenient to make the variables dimensionless. To accomplish this step, we may introduce a representative length scale a, where a is the radius of the subsurface sphere. The following dimensionless variables and quantities have been chosen for computation: the wave number of non-diffusive propagating waves is $ka = 0.01$–3.0, the relative length of thermal diffusion is $\mu/a = 0.10$–5.0, and the real and the imaginary parts of the nonhomogeneous parameter are $\sigma_1 a = 0.01$–1.0 and $\sigma_2 a = 0.01$–1.0, respectively. The ratio of embedded depth is $b/a = 1.1$–3.0, and the ratio of temperature is ϑ/ϑ_0.

Thus, the dimensionless complex wave number $\kappa a = \alpha a + \mathrm{i}\beta a$ is written as

$$\alpha a = \sqrt{\sqrt{\frac{1}{4}[(ka)^2 - (\sigma_1 a)^2 + (\sigma_2 a)^2]^2 + \left[\left(\frac{a}{\mu}\right)^2 - (\sigma_1 a)(\sigma_2 a)\right]^2} + \frac{1}{2}[(ka)^2 - (\sigma_1 a)^2 + (\sigma_2 a)^2]}. \tag{27}$$

$$\beta a = \sqrt{\sqrt{\frac{1}{4}[(ka)^2 - (\sigma_1 a)^2 + (\sigma_2 a)^2]^2 + \left[\left(\frac{a}{\mu}\right)^2 - (\sigma_1 a)(\sigma_2 a)\right]^2} - \frac{1}{2}[(ka)^2 - (\sigma_1 a)^2 + (\sigma_2 a)^2]}. \tag{28}$$

According to Eq. (26), the temperature and phase difference at the surface of the semi-infinite exponentially graded material can be obtained. Fig. 2 illustrates the temperature distribution at the surface of the material with parameters: $ka = 0$, $\sigma_2 = 0$, $\mu/a = 0.5463$, and $b/a = 1.10$, which corresponds to the case of pure heat diffusion and the case without wave motion terms in the equation of heat conduction in homogeneous materials. From Fig. 2, it can be seen that the computing results of the temperature at the surface of the semi-infinite material show good agreements with those in the literature [15]. In this case, the thermal diffusivity is given by $D = 75\,\mathrm{mm}^2/\mathrm{s}$, the radius of the sphere defect is $a = 2.0\,\mathrm{mm}$, the embedded depth is $b = 2.2\,\mathrm{mm}$. It should be noted that the greater the relative length of thermal diffusion, the greater variation the temperatures, comparing with the classical theory of the heat conduction, display. At the location of $(0, 0, -b)$, the temperature reaches the maximum.

The phase difference at the surface of the semi-infinite material with parameters: $\sigma_2 a = 0$, $\mu/a = 0.5463$, $ka = 0$, $b/a = 1.1$ is illustrated in Fig. 3. It can be seen that the phase difference first increase with y, then reaches the maximum and approaches to zero as y further increases. Note that the maximum phase difference is near the edge of the embedded sphere. The variation

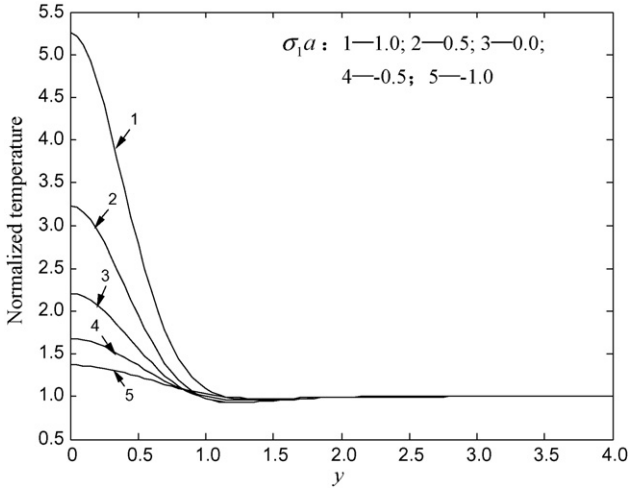

Fig. 2. Temperature distribution at the surface of the semi-infinite material ($\sigma_2 a = 0$, $ka = 0$, $\mu/a = 0.5463$, $b/a = 1.1$).

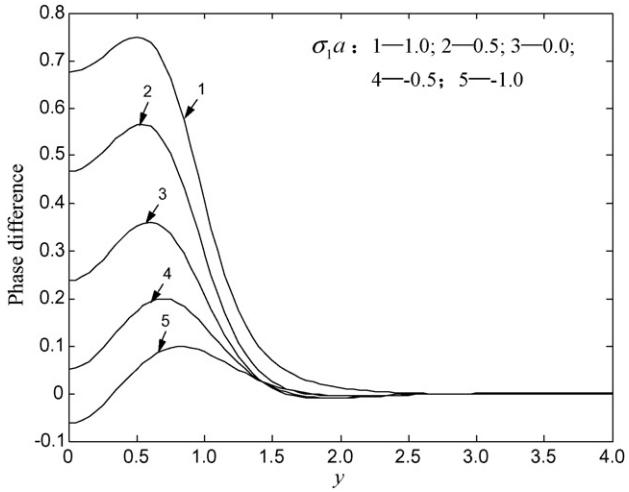

Fig. 3. Phase difference at the surface of the semi-infinite material ($\sigma_2 a = 0$, $\mu/a = 0.5463$, $ka = 0$, $b/a = 1.1$).

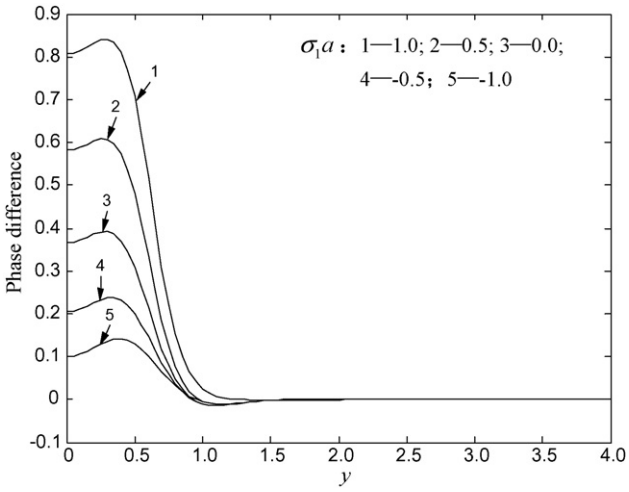

Fig. 5. Phase difference at the surface of the semi-infinite material ($\sigma_2 a = 0$, $\mu/a = 0.25$, $ka = 0$, $b/a = 1.1$).

of phase difference with nonhomogeneous parameter is great at the position near the center of the subsurface sphere defect. One can also see that the maximum phase difference increases with the increase of nonhomogeneous parameter.

The temperature distribution at the surface of the material with parameters: $\sigma_2 a = 0$, $b/a = 1.1$, $ka = 0$, $\mu/a = 0.25$ is depicted in Fig. 4. The numerical results show that when the wave number is comparatively little (e.g., $ka < 0.5$), the wave nature of heat conduction is weaker. The computing results of temperature are almost the same as those obtained by using the classical equation of heat conduction. So, the equation of thermal diffusion can be employed in engineering. When the wave number is comparatively large (e.g., $ka > 0.5$), the wave nature of heat conduction begins to have great effect on the amplitude of temperature.

The phase difference at the surface of the semi-infinite material with parameters: $\sigma_2 a = 0$, $\mu/a = 0.25$, $ka = 0$, $b/a = 1.1$ is illustrated in Fig. 5. In contrast to Fig. 3, it can be seen that the maximum phase difference increases with the decrease of μ/a, and its location also changes.

The temperature distribution at the surface of the material with parameters: $\sigma_1 a = 0.5$, $\sigma_2 a = 0$, $b/a = 1.1$, $\mu/a = 0.5$ is depicted in Fig. 6. As can be seen in Fig. 6, only when the relative length of thermal diffusion is comparatively little and the wave number ka is comparatively large, the incident wave number has great effect on the temperature distribution. That is to say, when the length of thermal diffusion in materials is comparatively little or the characteristic dimension of defect is comparatively great, the wave nature in heat conduction can be ignored.

The phase difference at the surface of the semi-infinite material with parameters: $\sigma_1 a = 0.5$, $\sigma_2 a = 0$, $\mu/a = 0.5$, $b/a = 1.1$, is illustrated in Fig. 7. It can be seen that the maximum phase difference increases with the increase of dimensionless wave number. The variation of phase difference with dimensionless wave number is great at the position near the surface of the sphere defect.

Shown in Fig. 8 is the temperature distribution at the surface of the material with parameters: $\sigma_1 a = -0.5$, $\sigma_2 a = 0$, $\mu/a = 0.5$,

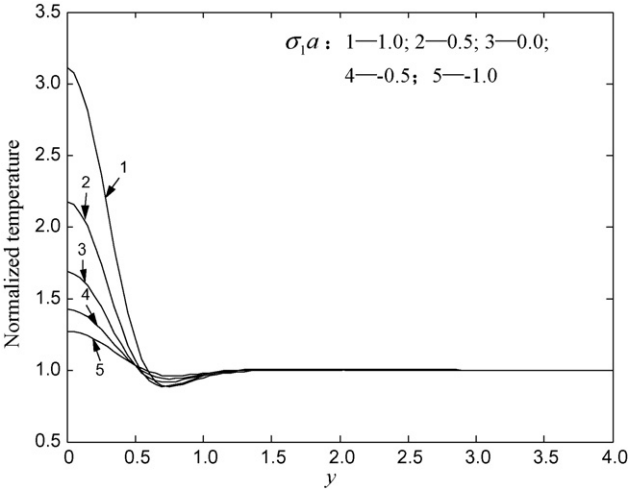

Fig. 4. Temperature distribution at the surface of the semi-infinite material ($\sigma_2 a = 0$, $\mu/a = 0.25$, $ka = 0$, $b/a = 1.1$).

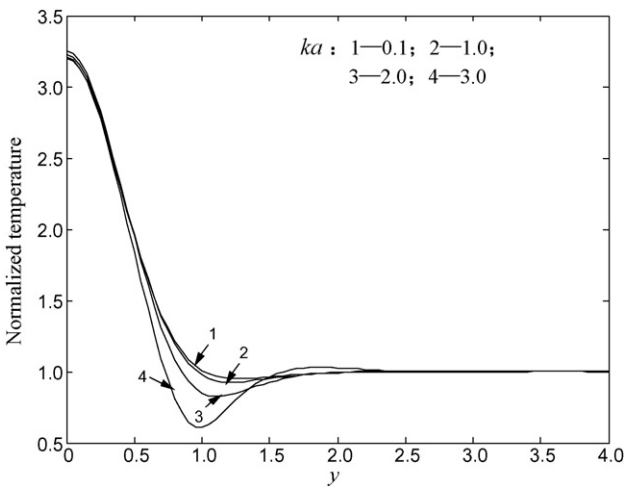

Fig. 6. Temperature distribution at the surface of the semi-infinite material ($\sigma_1 a = 0.5$, $\sigma_2 a = 0$, $b/a = 1.1$).

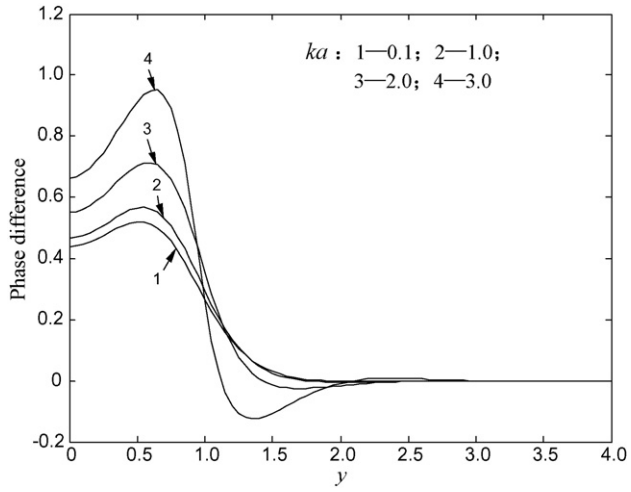

Fig. 7. Phase difference at the surface of the semi-infinite material ($\sigma_1 a = 0.5$, $\sigma_2 a = 0$, $\mu/a = 0.5$, $b/a = 1.1$).

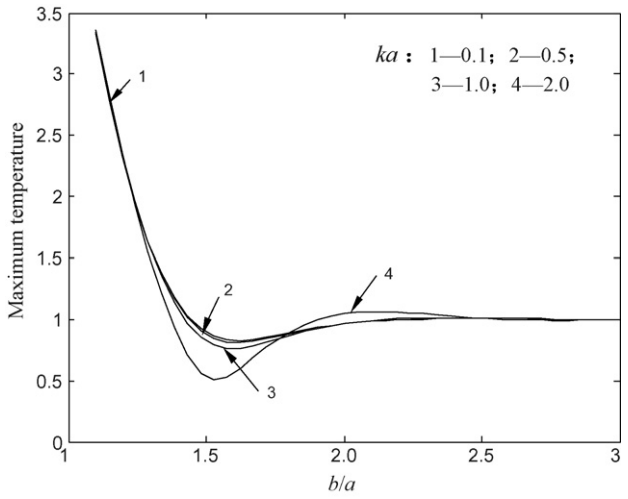

Fig. 9. Maximum temperature at the surface as a function of embedded depth ($\sigma_1 a = 0.5$, $\sigma_2 a = 0$, $\mu/a = 0.5$).

$b/a = 1.1$. According to Fig. 8, when the embedded depth is comparatively great, the variational amplitude of temperature is little. It is worth noting that when the wave number ka is comparatively small, the influence of wave nature in heat conduction is weaker. Results for effect of dimensionless wave number on the maximum temperature as a function of the embedded depth are presented in Fig. 9. It can be seen that when the diffusive length is comparatively great or the dimension of defect is comparatively little, the wave nature of thermal waves has great effect on the maximum temperature. If the wave number of heat conduction is comparatively large, or the frequency is comparatively high, the wave nature of thermal waves has the property of particle. It is also clear that the effect of dimensionless wave number on the maximum temperature is greater when the value of b/a is near 1.5. If the value of b/a is greater than 3.0, the effect of dimensionless wave number tends to be vanish.

The temperature distribution at the surface of the material as a function of dimensionless wave number is illustrated in Figs. 10 and 11. It is shown in Figs. 10 and 11 that when

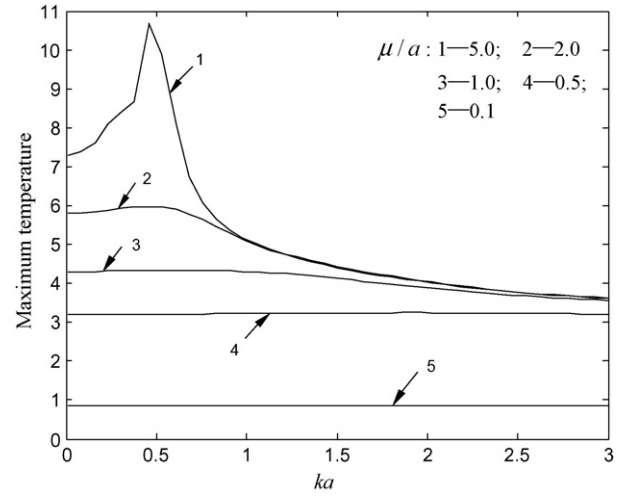

Fig. 10. Maximum temperature at the surface as a function of wave number ($\sigma_1 a = 0.5$, $\sigma_2 a = 0$, $b/a = 1.1$).

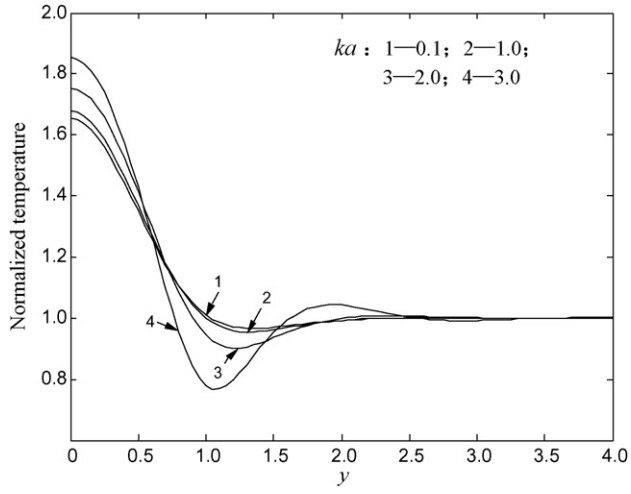

Fig. 8. Temperature distribution at the surface of the semi-infinite material ($\sigma_1 a = 0.5$, $\sigma_2 a = 0$, $\mu/a = 0.5$, $b/a = 1.1$).

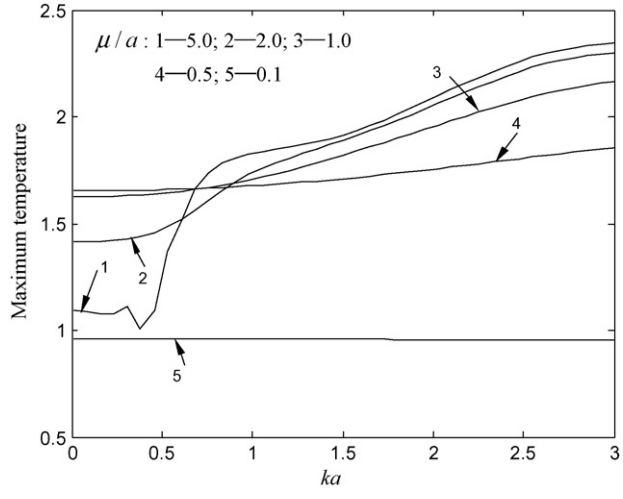

Fig. 11. Maximum temperature at the surface as function of embedded depth ($\sigma_1 a = -0.5$, $\sigma_2 a = 0$, $b/a = 1.1$).

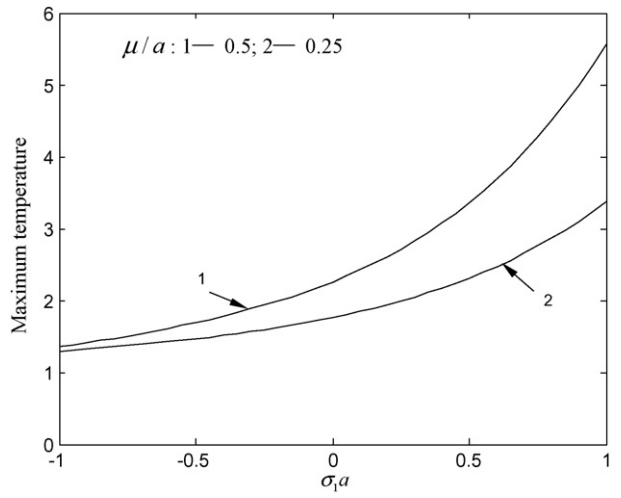

Fig. 12. Maximum temperature at the surface of materials as a function of nonhomogeneous parameter ($b/a = 1.1$, $ka = 1.0$, $\sigma_2 = 0$).

the nonhomogeneous parameter of the FGMs is positive, and the wave number is comparatively small, the wave nature of heat conduction has great effects on the distribution of temperature. Conversely, if the wave number is comparatively large, the effects of wave nature of heat conduction on the distribution of temperature tend to vanish. The maximum temperature distribution on the surface of the semi-infinite material as a function of nonhomogeneous parameter is illustrated in Fig. 12. It can be seen from Fig. 12 that the maximum amplitude of temperature on the surface of the material increases with the increase of the nonhomogeneous parameter. The maximum amplitude increases greatly when the nonhomogeneous parameter of FGMs varies from the negative to positive value. The variation of maximum amplitude with nonhomogeneous parameter increases with the increase of μ/a.

6. Conclusions

Applying the non-Fourier law of heat conduction, a theoretical study of the thermal wave propagation in a semi-infinite material with an embedded sphere defect has been considered, a general solution for the scattered field of thermal waves is presented. In contrast to the results in previous literatures [15], it can be concluded that the hyperbolic heat conduction equation cannot be regarded as a continuation of the parabolic heat conduction equation at very short time scale. When the propagating speed of thermal waves is $c \to \infty$ and the nonhomogeneous parameter is $\sigma \to 0$, the non-Fourier's wave model of heat conduction in FGMs is reduced to the classical model of Fourier's thermal diffusion. In fact, the nonhomogenous parameter is also taken as complex variable, namely, $\sigma_2 \neq 0$. Without loss of generality, we just investigate the thermal wave scattering of subsurface sphere and give the numerical results when the nonhomogenous parameter is $\sigma_1 \neq 0$ $\sigma_2 = 0$.

Through numerical examples, the distribution and variation of the temperature amplitude and phase difference under different parameters are analyzed. It has been found that on the illuminated side of the embedded sphere defect, the variational amplitude of temperature reaches the maximum. When the length of thermal diffusion is comparatively great, or the characteristic dimension of defect is comparatively little, the effect of the wave nature in thermal conduction on the temperature becomes great. When the modulated frequency of the incident thermal waves is greater than a certain number (that is relative to short waves), the wave nature of thermal waves begins to have great effects on the temperature amplitude and phase difference. We can also find that the maximum phase difference increases with the increase of nonhomogeneous parameter and dimensionless wave number. The results of this paper can provide theoretical foundation and references for the detection of defects by using laser heating, the inverse problem, and the analysis of infrared thermal imaging.

Acknowledgements

The work is supported by the National Natural Science Foundation of China (Foundation No.10572045). The authors are grateful to the anonymous reviewers for their constructive comments and suggestions.

References

[1] A. Mandelis, Diffusion Wave Fields: Mathematical Methods and Green Functions, Springer, 2001.
[2] M.J. Mourer, H.A. Thompson, J. Heat Trans. 95 (1973) 284.
[3] D.W. Tang, N. Araki, Int. J. Thermophys. 18 (1997) 493.
[4] J. Aboudi, M.-J. Pindera, S.M. Arnold, Compos. Part B-Eng. 30 (1999) 777.
[5] L.J. Gray, T. Kaplan, J.D. Richardson, ASME J. Appl. Mech. 70 (2003) 543.
[6] V. Peshkov, Second sound in helium II, J. Phys. 8 (1944) 381.
[7] C. Cattaneo, CR Phys. 247 (1958) 431.
[8] T.Q. Qiu, C.L. Tien, Int. J. Heat Mass Trans. 35 (1992) 719.
[9] D.Y. Tzou, ASME J. Heat Trans. 117 (1995) 8.
[10] C. Korner, H.W. Bergmann, Appl. Phys. A 67 (1998) 397.
[11] J.M. Terron, A. Sanchez-Lavega, A. Salazar, J. Appl. Phys. 87 (2000) 2600.
[12] J.B. Thibaud, R. Carminati, J.J. Greffet, J. Appl. Phys. 87 (2000) 7638.
[13] J.M. Terron, A. Sanchez-Lavega, A. Salazar, J. Appl. Phys. 89 (2001) 5696.
[14] A. Salazar, A. Sanchez-Lavega, J. Appl. Phys. 93 (2003) 4536.
[15] F. Garrido, A. Salazar, J. Appl. Phys. 95 (2004) 140.
[16] Bishri Abdel-Hamid, Appl. Math. Model. 23 (1999) 899.
[17] P.M. Morse, K.U. Ingard, Theoretical Acoustics, McGraw-Hill, New York, 1968.
[18] N.B. Kakogiannos, J.A. Roumeliotis, J. Acoust. Soc. Am. 98 (1995) 3508.
[19] M.A. Abramowitz, I.A. Stegun, Handbook of Mathematical Functions, National Bureau of Standards, Washington, DC, 1964.